Nanotechnology

Principles of conjugating quantum dots to proteins via carbodiimide chemistry

To cite this article: Fayi Song and Warren C W Chan 2011 *Nanotechnology* **22** 494006

Nanotechnology **22** (2011) 494006 (7pp) doi:10.1088/0957-4484/22/49/494006

Principles of conjugating quantum dots to proteins via carbodiimide chemistry

Fayi Song and Warren C W Chan

Institute of Biomaterials and Biomedical Engineering, Donelly Center for Cellular and Biomolecular Research, Materials Science and Engineering, Chemical Engineering, Chemistry, University of Toronto, Toronto, ON, M5S 3G9, Canada

E-mail: warren.chan@utoronto.ca

Received 7 June 2011, in final form 25 July 2011
Published 21 November 2011
Online at stacks.iop.org/Nano/22/494006

Abstract
The covalent coupling of nanomaterials to bio-recognition molecules is a critical intermediate step in using nanomaterials for biology and medicine. Here we investigate the carbodiimide-mediated conjugation of fluorescent quantum dots to different proteins (e.g., immunoglobulin G, bovine serum albumin, and horseradish peroxidase). To enable these studies, we developed a simple method to isolate quantum dot bioconjugates from unconjugated quantum dots. The results show that the reactant concentrations and protein type will impact the overall number of proteins conjugated onto the surfaces of the quantum dots, homogeneity of the protein–quantum dot conjugate population, quantum efficiency, binding avidity, and enzymatic kinetics. We propose general principles that should be followed for the successful coupling of proteins to quantum dots.

S Online supplementary data available from stacks.iop.org/Nano/22/494006/mmedia

(Some figures may appear in colour only in the online journal)

1. Introduction

The successful coating of quantum dots with biological molecules is important for their utility in biology and medicine. These biological molecules enable the quantum dots to specifically target molecules, cells, tissues, and organs for diagnostic and therapeutic applications [1–7]. Gao *et al* [8] coated quantum dots with prostate specific monoclonal antibodies for *in vivo* targeting of prostate tumors in xenograft animals. Both Wu *et al* [9] and Ghazani *et al* [10] conjugated quantum dots with antibodies to detect cancer biomarkers on cells and tissues respectively. Beyond quantum dots, conjugation chemistry is also commonly used to link other types of nanomaterials (e.g., gold nanoparticles, magnetic nanoparticles) to bio-recognition molecules. While there has been a significant amount of research on the synthesis of nanomaterials and their surface modifications to render them water-soluble and biocompatible [11–15], there has been limited research effort in understanding and optimizing the reaction conditions to covalently link nanomaterials such as quantum dots to bio-recognition molecules. Although this is an intermediate step in the final use of nanomaterials in biomedical research and applications, the conjugation reaction step could dictate the success of the end biomedical experiment. Here we characterized the carbodiimide chemistry of linking water-soluble ZnS-capped CdSe quantum dots with proteins in order to develop quality control for measuring the final quantum dot bioconjugates. We decided to focus on carbodiimide chemistry because it is the most prevalent conjugation strategy used in nanotechnology today. Carbodiimide molecules commonly react with carboxylic acids to form an acylisourea intermediate that is subsequently displaced by primary amines to form an amide bond that covalently links two entities (e.g., nanoparticle with protein).

2. Materials and methods

2.1. Reagents and equipment

Tri-*n*-octylphosphine oxide (TOPO, tech. 90%), selenium powder (Se, 99.5%), hexamethyldisilathiane (Bis(trimethylsilyl) sulfide $(TMS)_2S$), trioctylphosphine (TOP, tech. 90%), polyacrylic acid, agarose, 1-ethyl-3-(3-dimethylaminopropyl) carbodiimide (EDC) and *N*-hydroxysulfosuccinimide (sulfo-NHS), dimethylformamide (DMF), bovine serum albumin (BSA), stabilized horseradish peroxidase (HRP), human

immunoglobulin (IgG), and anti-IgG were purchased from Sigma-Aldrich. Dimethylcadmium (DMC, min 97%) and diethylzinc (DEZ, min 95%, 10 wt% in hexane) were purchased from Strem Chemicals. Chloroform, methanol, and acetone (ACS grade) were purchased from EMD Chemicals Inc. 10× tris-borate-EDTA electrophoresis buffer (TBE) was purchased from Fermentas. 3,3′, 5,5′-tetramethylbenzidine (TMB) dichloride was purchased from Bioshop. Ready-to-use ELISA TMB substrates were purchased from eBioscience.

Absorbance spectra were recorded with a UV–vis spectrophotometer (Shimadzu, UV-1601PC). A spectrofluorometer (Spex FluroMax-3, Jobin Yvon) was used to characterize the fluorescent properties of the quantum dots and their conjugates. A SUNRISE microplate reader was used for ELISA measurements.

2.2. Synthesis and preparation of water-soluble quantum dots

Organic-soluble quantum dots were first synthesized based on previously reported methods [20, 21] with minor modifications. Amphiphilic polymer, 40% ODA-PAA, and the amphiphilic polymer coated quantum dots, PQD, were prepared in our laboratory based on a previously developed method [15]. Briefly, CdSe cores were obtained from a mixture of TOP/Se and DMC in TOPO solvent at 320 °C. The temperature was then decreased to 270 °C and ZnS precursor solution (DEZ, TOP, and $(TMS)_2S$) was added to the reaction flask to form a ZnS capping shell on the surface of the CdSe. These quantum dots were purified by size-selective precipitation and were then dissolved in chloroform. To water-solubilize them, they were mixed with amphiphilic polymers (40% octylamine and 60% polyacrylic acid), sonicated, and then dried to remove the chloroform. Deionized water was added and the pH was adjusted to 11 with NaOH to dissolve the solid pellets. Then the sample was filtered with a syringe filter (0.22 μm) to remove any aggregation. Finally, the concentrated sample was purified through a Sephadex G25 gel column using borate buffer (BB) at pH 9.0 as the elution solution. The collected sample was stored at room temperature prior to use in protein conjugation.

2.3. Covalent conjugation of quantum dots to proteins

The conjugation of protein with PQDs using EDC as a catalyst was conducted. We systematically varied the stoichiometry of the reactants and catalysts in order to determine the effect of EDC on the final PQD–protein conjugate. The conditions are described in each figure. Sulfo-NHS was also added into the reaction since NHS has been known to stabilize the EDC intermediate but the concentration of sulfo-NHS was not changed in the reaction. Briefly, the PQD solution was mixed with sulfo-NHS first and then EDC was added to the reaction vessel. After approximately 2 min, a solution of proteins was added, followed by incubation for 2–3 h at room temperature with gentle shaking. All conjugation reactions occurred at pH 7.4 in borate buffer unless otherwise specified.

After finishing the conjugation reaction, electrophoresis using agarose gel (0.8% in 0.5× TBE) was employed to characterize the conjugates. The electrophoresis conditions were 0.5× TBE at 50 V for 50–60 min. Fluorescence images of the gel were obtained using BioRad Gel Doc XR (Hercules, CA) with UV light. The desired bands were removed by scalpel from the gel slab under UV light, and were collected and homogenized in centrifuge tubes. Afterward, the tube was placed in an ethanol–dry ice bath for at least 10 min to ensure that the gel was frozen, followed by thawing at room temperature for 30 min. Finally, the sample was centrifuged at 3000 rpm for 3 min to pellet the gel fragments and the supernatant was collected. This freeze–thaw process was repeated one or two more times. The collected QD bioconjugates solution was filtered with a syringe filter (0.22 μm) to remove gel fragments and the sample was stored at 4 °C prior to further analysis.

2.4. Determining the number of proteins on the surfaces of the quantum dots

To confirm the binding activity of the human IgG conjugated with PQD, ELISA was used. Human IgG ELISA kits were purchased from Immunology Consultants Laboratory and the protocols from the company were followed. Briefly, the human IgG–PQD conjugates solution was loaded into the ELISA plates, incubated for 60 min at room temperature, followed by washing buffer (supplied in the kit) and then 20 min incubation with HRP conjugated anti-human IgG Fc antibody in a stabilizing buffer. After a thorough rinse, substrate solution provided with the kits was added into each well and after 10 min a stop solution was added to produce a yellow color for positive detection. The signal intensity was measured using a spectrophotometer (absorbance at 450 nm).

The number (N) of proteins bound to the PQD surface was determined by comparing the molar concentrations of proteins (C_p) and QDs (C_q) of the purified protein–PQD conjugates, i.e., $N = C_p/C_q$. The concentration of proteins was measured with the ELISA kit as described above. A standard calibration curve is created and compared to the ELISA from the PQD coated with the protein to determine the number of proteins bound to the PQD surface. The concentration of PQDs was determined by measuring the spectrophotometric absorbance at peak wavelength using Beer's law ($A = ebc$) and using the molar absorptivity coefficient of 91 441 M^{-1} cm^{-1} to determine the number of PQDs.

2.5. Determining the binding avidity of IgG on the quantum dots

We used the technique of Bobrovnik *et al* [22] to determine the binding avidity (K_d) of the IgG on the PQD. In this technique the K_d is determined from the following equation:

$$(A_0 - A_i)/A_i = K_a l_i \quad (1)$$

$$K_d = 1/K_a. \quad (2)$$

K_a is the affinity constant of the IgG–PQD conjugate, l_i is the variable concentration of antigen (i.e., the anti-human IgG antibody), and A_0 and A_i are the absorbances of microwells containing only IgG–PQD conjugates and the mixture of IgG–PQD conjugates and anti-human IgG (l_i) at equilibrium.

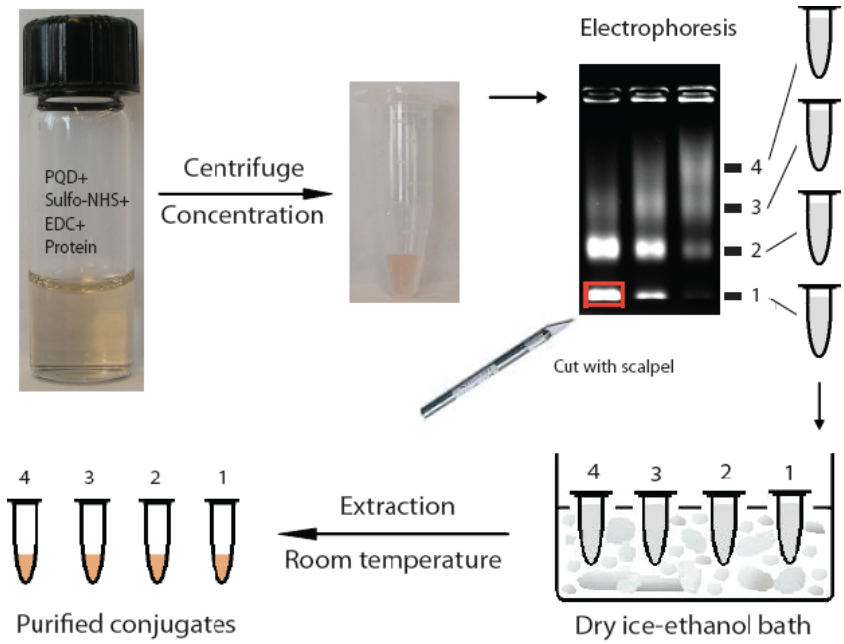

Figure 1. Schematic of the bioconjugation and purification of polymer coated quantum dots (PQDs) with proteins.

Experimentally, IgG–PQD conjugates (isolated from the wells) were incubated with various amounts of anti-human IgG (final concentration l_i) for 18 h in a centrifuge tube, which allowed the binding interactions to reach equilibrium. Afterward, the equilibrated mixture solution was loaded into the anti-human IgG pre-coated microplate well for ELISA measurements as described above. K_a values for different conjugates could be obtained from the slope of a plot of $(A_0 - A_i)/A_i$ against l_i, as shown in figure S1 (available at stacks.iop.org/Nano/22/494006/mmedia).

2.6. Determining the enzyme kinetics of HRP on the quantum dots

The HRP kinetics was studied in a 96 well microplate at room temperature in 10 mM phosphate buffer (pH 6.2). The isolated HRP–PQDs were placed in 96 well microplates at room temperature in 10 mM phosphate buffer (pH = 6.2) and a varying concentration of TMB (dissolved in 10% DMF) was added to the reaction well. Afterward, hydrogen peroxide was added to the different wells and the absorbance signal was recorded at 655 nm. A Lineweaver–Burk plot was applied to obtain the kinetic parameters as shown in S2 (available at stacks.iop.org/Nano/22/494006/mmedia).

3. Results and discussion

We systematically examined the conjugation of proteins onto the surface of ZnS-capped CdSe quantum dots coated with amphiphilic polymers (denoted as PQDs). Figure 1 provides the overall experimental scheme. In these experiments, we incubated PQDs with the water-soluble carbodiimide 1-ethyl-3-(3-dimethylaminopropyl)carbodiimide (denoted as EDC) and sulfo-*N*-hydroxylsuccinimide esters (sulfo-NHS) with defined concentrations of PQDs and proteins. The purpose of the sulfo-NHS is to stabilize the intermediate by preventing it from being attacked by water molecules. As a first step, we confirmed that proteins were indeed conjugated onto the surfaces of the PQDs. IgG and PQDs were reacted together with EDC and confirmed by using gel electrophoresis. We imaged the gel by fluorescence and then we stained the gel using the protein-binding dye molecule Coomassie blue. A comparison of the fluorescence and color images of the gel shows regions of co-staining, suggesting that the protein and PQDs were indeed conjugated. At the edge of the gel, we observed PQDs not stained with Coomassie blue, indicating bands of unconjugated PQDs. Also, unconjugated proteins migrated in a different direction from the PQD–IgG conjugates. See figures 2(A) and (B).

Next, we characterized the effect of EDC concentration on the final PQD–protein conjugates. The concentrations of the PQDs and protein immunoglobulin G (IgG) were kept constant while we altered the concentration of EDC. The results are shown in figure 2(C). The electropherogram shows that at a defined EDC concentration (16–62 times excess to the PQD concentration), we observed the PQD bioconjugate as a relatively homogeneous population. This is depicted by the intense fluorescence signal from band 2. The reaction efficiency is strongly dependent upon the amount of EDC used in the study. Band 1 shows PQDs that are unconjugated. The percentage of unconjugated PQDs decreased with increase of the EDC-to-PQD ratio (figure 2(D)). In the range of 16–62 EDC-to-PQD ratio, we observed an increase in the formation of PQD conjugates (see figure 2).

Using enzyme-linked immunosorbent assays (ELISA), we determined that the PQDs in band 2 contained one IgG protein per PQD. As we increased the EDC concentration, we observed a heterogeneous PQD–IgG population where two or

(A)

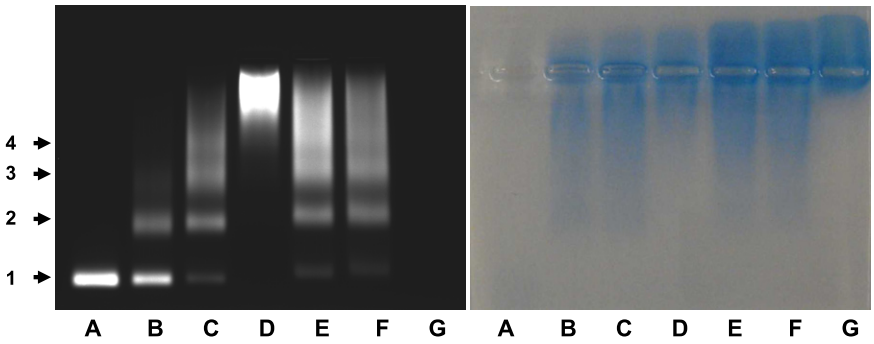

(B)

Sample	A	B	C	D	E	F	G
Concentration of PQD (nM)	200	200	200	200	200	200	0
Concentration of IgG (nM)	0	2000	4000	8000	8000	8000	8000
IgG/PQD molar ratio	0	10	20	40	40	40	0
EDC/PQD molar ratio	0	500	500	500	250	100	0

(C)

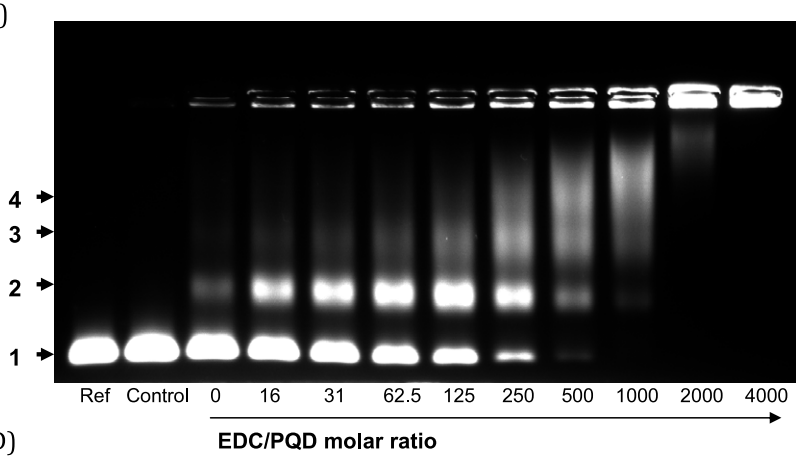

(D)

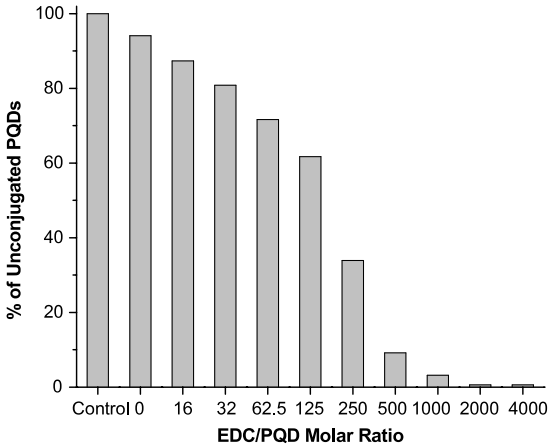

Figure 2. Coomassie blue staining and fluorescence imaging verified conjugation of IgG onto PQDs. Conjugation of human IgG to PQDs. (A) Fluorescence image (left) and colorimetric image (right) after Coomassie stain for the PQDs and their conjugates in a gel after electrophoretic separation. (B) Reaction concentrations of the IgG, EDC, and PQDs. (C) Electropherogram of human IgG–PQD conjugates at different EDC/PQD molar ratios. The IgG/PQD molar ratio is fixed at 20. Ref denotes pure PQDs only and Control represents PQDs with EDC addition (EDC/PQD ratio 500, but no IgG). (D) Percentage of unconjugated PQDs for each EDC/PQD molar ratio. To obtain a percentage, the intensity, as measured by the software Image J, of band 1 for different EDC/PQD ratios is divided by the intensity of the 'Ref' band 1.

(A)

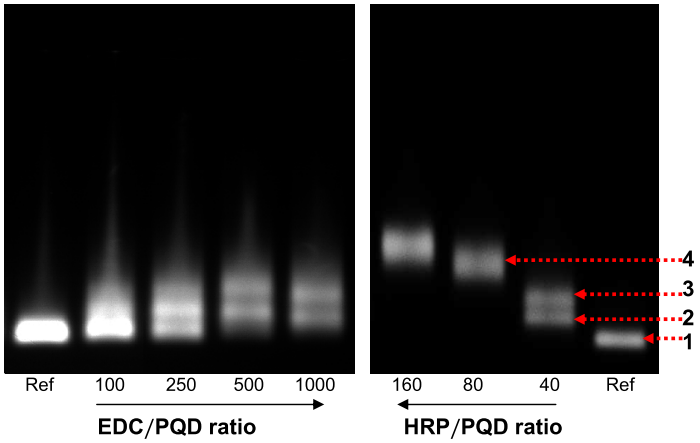

(B)

Sample	A	B	C	D	E	F	G	H	I
Concentration of PQD (nM)	150	150	150	150	150	150	150	150	150
Concentration of HRP (nM)	0	6000	6000	6000	6000	24000	12000	6000	0
HRP/PQD molar ratio	0	40	40	40	40	160	80	40	0
EDC/PQD molar ratio	0	100	250	500	1000	1000	1000	1000	0

Figure 3. Conjugation of HRP to PQDs. (A) Images of HRP–PQDs conjugated with different EDC (left) and HRP (right) concentrations. Ref represents PQDs without HRP. Based on the results of IgG, the HRP/PQD molar ratio was fixed to 40 for the left panel, and the EDC/PQD molar ratio was fixed to 1000 for the right panel. (B) Reaction concentrations of the HRP, PQDs, and EDC.

more IgGs were coated onto the surface. With excess EDC, we observed massive aggregation of the PQDs as shown by the fluorescence signal at the well. The ability to place various amounts of IgGs on the PQDs could significantly impact their biological applicability. It has been demonstrated that the coating of multiple proteins on a nanoparticle surface could alter their avidity to the target and could have implications in binding kinetics and cellular response [16–18]. Additionally, the homogeneity of the PQD–protein population is dependent upon the protein and the EDC concentration. In figure 3, we show that the electrophoretic profile of the protein horseradish peroxidase is different from that for IgG. In these experiments, the migration distance from the gel electrophoresis experiment was not significantly different for QD–HRP conjugates using an EDC/PQD ratio below 100 and therefore the results are not presented. Also, the concentration of EDC for covalently conjugating horseradish peroxidase to PQDs is also different from that for IgG. This is likely due to the different amount of available primary amines on the protein for conjugation and also the non-specific adsorption of proteins onto the PQD surface is dependent upon the protein. Furthermore, the concentration of the HRP to PQDs also influences the final homogeneity of the PQD–HRP conjugate population (see figure 3). These results suggest that researchers need to systematically optimize the reaction stoichiometry of the protein, PQDs and EDC for different biomolecules in order to obtain a homogeneous PQD conjugate sample.

Purification of the PQD–protein conjugates is achieved by using a freeze–thaw method. Electrophoresis is able to separate the conjugates with different amount of proteins on the PQD surface. In our method, the band was removed using a scalpel under UV-illumination, homogenized, and the band was then frozen in a dry ice–ethanol bath for 10 min. The pores in the gel increase in size during this freeze–thaw process enabling the PQD–protein conjugates to diffuse into solution. The PQD–protein conjugates are clearly visible in solution under UV-illumination. For some PQD–protein conjugates, this process may require repetition since the final size of the PQD–protein conjugate depends on the EDC concentration and the sizes of the proteins and PQDs. For example, PQDs coated with the protein bovine serum albumin (BSA) required three extractions to isolate most of the PQD–BSA conjugates. We recovered 55% in the first round, another 26% in the second round for a total of 81%, and 14% more in the final round for a total of 95% (figure S3 available at stacks.iop.org/Nano/22/494006/mmedia). This method is rapid in comparison to soaking homogenized gels in buffer which requires three days to extract the conjugate from the gel [19]. This purification technique could be used to isolate protein conjugated PQDs from unconjugated PQDs.

We next examined the properties of the PQDs and proteins after the conjugation. Isolating the PQD–IgG conjugates from the gel from the experiments depicted in figure 4, we measured the quantum efficiency of the PQD–protein conjugate. Interestingly, our results showed that PQDs with one IgG on their surface had a quantum efficiency of 15% but we observed a trend of an increase in quantum efficiency with an increase in the number of IgGs bound to the PQD

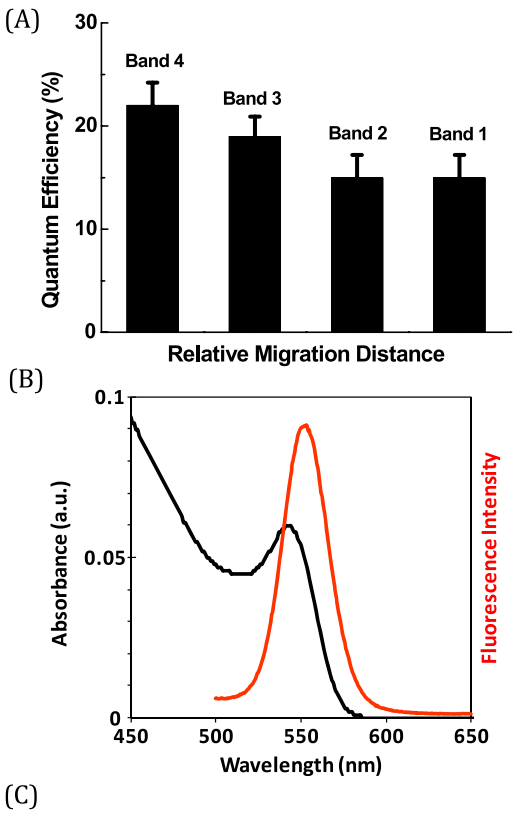

(C)

Sample	Pure IgG	Band 2	Band 3	Band 4
K_d (M)	6.2×10^{-10}	5.1×10^{-10}	7.7×10^{-10}	1.1×10^{-9}

Figure 4. Properties of the PQDs and IgGs post-conjugation. (A) Quantum efficiency for PQDs coated with different amounts of human IgG (bands 1–4). (B) Representative absorbance and fluorescence spectra of IgG–PQDs (band 3). (C) Binding avidity of the human IgG on the surfaces of the PQDs. These K_d values were determined using the method proposed by Brovnik [22].

surface. Other properties such as photostability, absorbance and fluorescence profile (see figure 4(B)) remained relatively the same before and after conjugation.

For the proteins on the surface of the PQDs, we characterized the binding avidity of the IgG and the enzyme activities of horseradish peroxidase. Figure 4(C) shows that the increase in the binding avidity of IgG on PQDs was not significantly changed when we used a lower amount of EDC for the conjugation reaction to produce PQDs with one to three IgG proteins on their surfaces. In contrast, when there were more than three proteins, we observed a decrease in the binding avidity (from 10^{-10} to 10^{-9} M). Normally when a nanoparticle surface contains more than one protein, we observe a multivalent effect where the binding of multiple proteins on a scaffold to the targets leads to a stronger interaction. In contrast, our results may suggest that EDC may non-specifically cross-link proteins and this impacts their binding avidity. Finally, the enzyme activities of the horseradish peroxidase were measured when it was covalently conjugated to PQDs. Figure 5 shows that the enzymatic activities of the horseradish peroxidase are heavily dependent on the amount of EDC used in the reaction.

Six Key Principles to Successfully Conjugating Proteins to QDs

Principle 1: Experiments must be systematically conducted to determine proper reactant concentrations to prevent or minimize aggregation of QD-conjugates.

Principle 2: Analytical techniques such as gel electrophoresis (aggregates are not mobile), fluorescence microscopy (lack of blinking), or electron microscopy should be used to monitor aggregation during the reaction.

Principle 3: Optical properties (fluorescence full width at half-maximum, absorbance, photobleaching, quantum yield) of QDs after protein conjugation may be altered and should be measured.

Principle 4: Binding or enzymatic properties of proteins may be altered after binding onto QDs and should be measured.

Principle 5: Unconjugated proteins should be removed from those conjugated onto the QD surface.

Principle 6: The number of proteins on QD surface should be measured and the overall size should be determined.

Figure 6. Principles of PQD conjugation to proteins. The figure depicts six basic principles that would ensure the formation of single and monodisperse quantum dot–protein conjugates.

4. Conclusion

We demonstrated that the successful conjugation of quantum dots to proteins requires careful systematic optimization. We showed that the concentrations of PQDs, proteins, and EDC can influence the reaction efficiency and number of proteins coated on the surfaces of the PQDs. Additionally the distribution of the number of proteins per PQD is also dependent on the experimental conditions. Hence, the final PQD–protein construct can influence the PQDs' quantum

Sample	Pure HRP (0.2nM)	Band 3 (2.0nM)	Band 4 (2.7nM)
K_m (mM)	1.2±0.2	1.0±0.5	1.0±0.5
V_{max} (mM s^{-1})	0.0010±0.0003	0.0010±0.0006	0.0033±0.0009
Normalized V_{max} (mM s^{-1}/nM)	0.0050±0.0015	0.0005±0.0001	0.0012±0.0003

Figure 5. Enzyme kinetics of HRP on PQDs. Enzymatic kinetic data obtained from PQD–HRP conjugates extracted from figure 3(A) (right gel). Band 1 corresponds to unconjugated PQD and did not show an enzymatic response. Band 2 shows very weak HRP enzymatic activity because we are not able to purify enough samples. Only data for pure HRP, bands 3 and 4 are presented in this table. The average values and confidence intervals are presented based on five experimental repetition experiments with the t-test at 90% confidence level ($X = \bar{X} \pm t(S_x/N^{1/2})$).

efficiency, the protein's binding avidity and the enzymatic activities. Our results clearly demonstrate the characterization of conjugation efficiency, assessment of PQD and protein properties, and isolation of PQD–protein conjugates from unconjugated PQDs is required before using them in biological and medical experiments. Figure 6 provides a general optimization principles for successfully conjugated quantum dots (or other types of nanoparticles) to proteins.

Acknowledgments

We would like to acknowledge the Canadian Institute of Health Research, Natural Sciences and Engineering Research Council of Canada, Canadian Foundation for Innovation, and Ontario's Ministry of Research and Innovation for funding the project.

References

[1] Kim B Y, Jiang W, Oreopoulos J, Yip C, Rutka J T and Chan W C W 2008 *Nano Lett.* **8** 3887
[2] Zrazhevskiy P and Gao X 2009 *Nano Today* **4** 414
[3] Han M, Gao X, Su J Z and Nie S 2001 *Nature Biotechnol.* **19** 631
[4] Medintz I L, Uyeda H T, Goldman E R and Mattoussi H 2005 *Nature Mater.* **4** 435
[5] Dubertret B, Skourides P, Norris D J, Noireaux V, Brivanlou A H and Libchaber A 2002 *Science* **298** 1759
[6] Giri S, Sykes E A and Jennings T L 2011 *ACS Nano* **5** 1580
[7] Murcia M J, Minner D E, Mustata G-M, Ritchie K and Naumann C A 2008 *J. Am. Chem. Soc.* **130** 15054
[8] Gao X, Cui Y, Levenson R M, Chung L W K and Nie S 2004 *Nature Biotechnol.* **22** 969
[9] Wu X, Liu H, Liu J, Haley K N, Treadway J A, Larson J P, Ge N, Peale F and Bruchez M P 2003 *Nature Biotechnol.* **21** 41
[10] Ghazani A A, Lee J A, Klostranec J, Xiang Q, Dacosta R S, Wilson B C, Tsao M S and Chan W C W 2006 *Nano Lett.* **6** 2881
[11] Bentzen E L, Tomlinson I D, Mason J, Gresch P, Warnement M R, Wright D, Sanders-Bush E, Blakely R and Rosenthal S J 2005 *Bioconjug. Chem.* **16** 7
[12] Jiang W, Mardyani S, Fischer H and Chan W C W 2006 *J. Mater. Chem.* **18** 872
[13] Lees E E, Nguyen T-L, Clayton A H A and Mulvaney P 2009 *ACS Nano* **3** 1121
[14] Yu W W, Chang E, Falkner J C, Zhang J, Al-Somali A M, Sayes C M, Johns J, Drezek R and Colvin V L 2007 *J. Am. Chem. Soc.* **129** 2871
[15] Anderson R E and Chan W C W 2008 *ACS Nano* **2** 1341
[16] Martos V, Castreño P, Valero J and de Mendoza J 2008 *Curr. Opin. Chem. Biol.* **12** 698
[17] Montet X, Funovics M, Montet-Abou K, Weissleder R and Josephson L 2006 *J. Med. Chem.* **49** 6087
[18] Jiang W, Kim B Y S, Rutka J T and Chan W C W 2008 *Nature Nanotechnol.* **3** 145
[19] Sperling R A, Pellegrino T, Li J K, Chang W H and Parak W J 2006 *Adv. Funct. Mater.* **16** 943
[20] Dabbousi B O, Rodriguez-Viejo J, Mikulec F V, Heine J R, Mattoussi H, Ober R, Jensen K F and Bawendi M G 1997 *J. Phys. Chem.* B **101** 9463
[21] Peng X, Schlamp M C, Kadavanich A V and Alivisatos A P 1997 *J. Am. Chem. Soc.* **119** 7019
[22] Bobrovnik S A 2003 *J. Biochem. Biophys. Methods* **57** 213